

FEM ANALYSIS OF HYBRID STRUCTURAL FRAMES WITH R/C COLUMNS AND STEEL BEAMS

Hiroshi NOGUCHI¹ And Kazuhiro UCHIDA²

SUMMARY

Two frame specimens with R/C columns and steel beams which had different beam-column joints were analyzed using nonlinear three-dimensional finite element method (FEM). One specimen had through-beam type of beam-column joints with Face Bearing Plates(FBP), and failure mode was beam yielding. The other specimen had through-beam type of beam-column joints with cover plates, and failure mode was joint shear failure. The analysis of the latter was conducted before the test to predict the behavior of the specimen. FEM analysis considering the interaction between reinforcing bars and concrete and between steel and concrete simulated the behaviors of the frame specimen well. The failure process and shear resisting mechanisms of different shaped beam-column joints (interior, exterior, interior-top, and corner) were grasped from the analytical results of the stress-strain relation of concrete elements, shear forces of beam-column joints, the contribution of shear resisting elements, and the deformation components, which were not obtained from the experiment.

INTRODUCTION

Hybrid structures (RCS) consisting of R/C columns and steel beams have been developed in Japan. The advantage of these structures is their exquisite combination of R/C columns and steel beams. Many experimental studies have been conducted mainly on the behavior of interior beam-column joints using cross-shaped specimens. However, there have been few experimental and analytical studies on the behavior of RCS frames. In this research, the nonlinear three-dimensional finite element analysis of a previous RCS frame test specimen has been conducted. It is effective for promoting a greater understanding of the behavior of the RCS frame to investigate them from analytical aspects. Because it is difficult from economical aspects to conduct a lot of experiments, the investigation by the finite element analysis is significant. The three-dimensional nonlinear FEM program that the authors developed was used in this research [Uchida, 1994, 1998].

MATERIAL MODELS [Uchida, 1998]

Concrete The orthotropic hypoelastic model based on the equivalent uniaxial strain concept by Darwin and Pecknold was used. As a failure surface under triaxial stresses, the five-parameter model developed by William and Warnke was used. As the basic uniaxial stress-strain relationship, a tension cut off was assumed at the tension zone after cracking. At the compression zone, the Saenz's equation was used in the ascending zone and a linear decrease was assumed in the descending zone after the maximum stress. The compressive reduction factor

that was developed by Noguchi et al. was considered for cracked concrete.

Reinforcing bar A stress-strain relationship was assumed to be bilinear.

Steel An isotropic hardening model based on von Mises yield criterion was used.

Interaction between concrete and re-bar Bond between concrete and re-bars was expressed by the bond link elements. As for the bond stress-slip relationship, the bilinear model proposed by Morita et al. was used.

¹ Dept of Design and Architecture, Faculty of Engineering, Chiba University, Japan Email: noguchi@archi.ta.chiba-u.ac.jp

² Fujita Corporation, Tokyo 151-8503, Japan E-mail: uchida@fujita.co.jp

Interaction between concrete and steel Interface elements were used between concrete and steel. For compressive normal stresses, the friction model based on the bond test results that were conducted by Kim and Noguchi was used. For tensile normal stresses, the normal and shear stresses were released when the normal stress was over $\sigma_p/100$.

ANALYSIS OF FRAME SPECIMEN WITH FBP

Reference Specimen

A frame specimen TB that was tested by Iizuka, Kasamatsu and Noguchi [Iizuka, 1997] was selected for the analysis. It was the only test specimen in which joint failure was designed in previous RCS frame tests. The shape of the specimen is shown in Figure 1. It was a 1/3 scaled two story, two bay RCS moment resisting frame specimen. The joint detail was a beam through type with face bearing plates (FBP). Under constant column axial loads, reversed cyclic lateral loads were applied to the beam end of the second story. Failure mode of the specimen was beam yielding, but interior beam-column joints were also damaged.

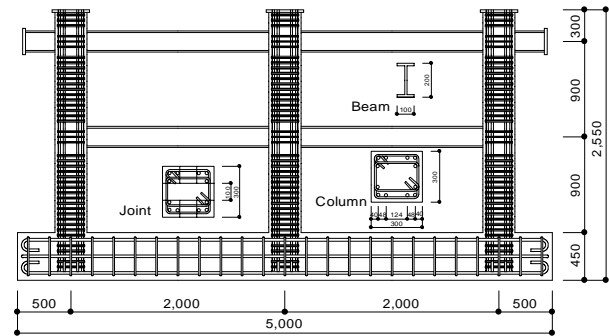


Figure 1: Shape of Specimen TB

Modeling of Specimen

The finite element idealization of the Specimen TB is shown in Figures 2 and 3. Half part of the specimen including the stub was modeled by using the symmetrical condition at the center in the direction of width. Three analytical cases were investigated. In Case 1, perfect bond was assumed both between re-bars and concrete and between steel and concrete. In Case 2, bond elements were used between re-bars and concrete. In Case 3, interface elements were used between steel and concrete in addition with Case 2. In Cases 2, 3, pulling out of column re-bars from the stub was considered by using bond link elements. Axial loads and monotonic lateral loads were applied to the specimen in the analysis.

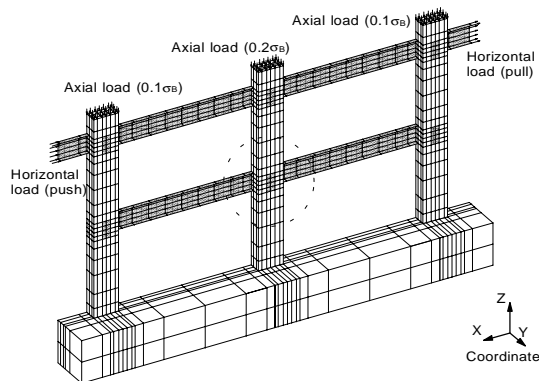


Figure 2: Finite Element Idealization

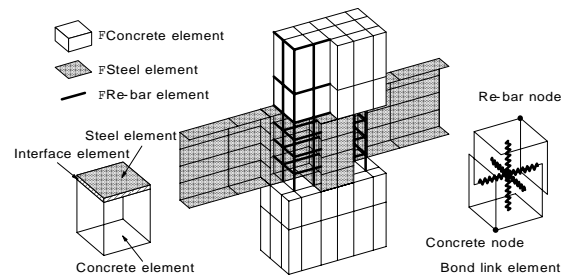


Figure 3: Detail of Beam-Column Joint

Analytical Results and Discussions

Load-deflection relationship

The relationship between lateral load and deformation is shown in Figure 4. The stiffness and the strength of Case1 were larger than those of the experiment. In Case 3, the result of analysis showed a good agreement with the experimental result. The load-deflection curve was influenced by the modeling of interaction between different kind materials such as concrete and re-bar, concrete and steel. In the later discussion, the analytical results of Case3 are used.

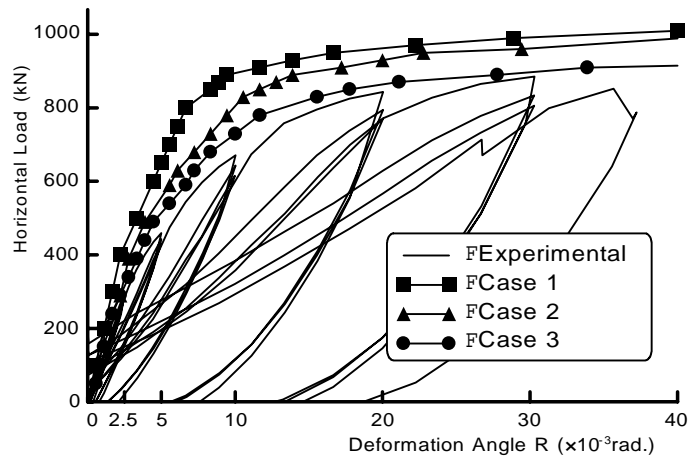


Figure 4: Load – Deflection Relationship

Minimum principal stress distribution in beam-column joints

Minimum principal stress distribution in beam-column joints is shown in Figure 5. The minimum principal stress of the interior beam-column joint is larger than that of the other joints. In each beam-column joint, the stress condition of two concrete parts (left and right sides) which were divided by the transverse steel beam was different. A compressive strut was formed from the outer concrete (out of the flange) to the inner concrete (in the flange) in the each joint area divided by transverse beams (allow line in Figure 5). It was found that the outer concrete also contributed to shear resisting.

Minimum principal stress-equivalent uniaxial strain relationship

It is necessary to verify the strain condition in order to investigate the concrete failure. The minimum principal stress-equivalent uniaxial strain relationships are shown in Figure 6. White symbols indicate the maximum strengths obtained from the equivalent uniaxial strain including crack width, black symbols indicate the minimum principal stresses. The maximum strengths depends on the compressive reduction factors corresponding to crack conditions. It was indicated that the middle and outer components of the interior beam-column joint failed in compression.

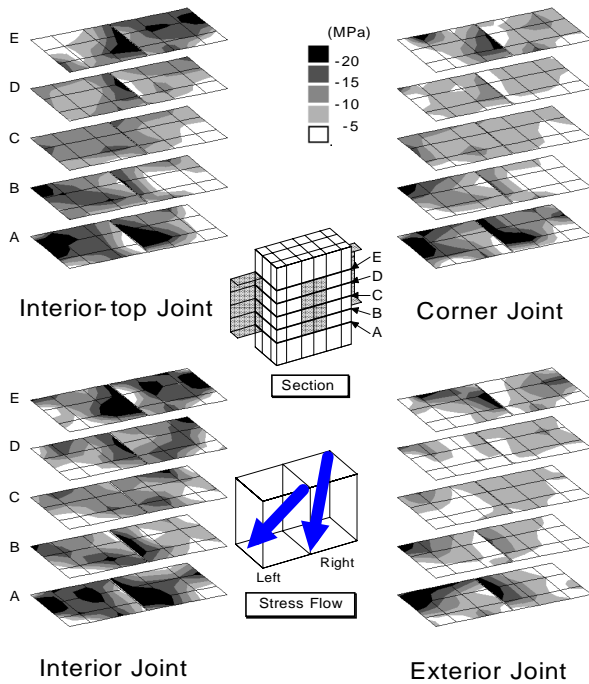


Figure 5: Distribution of Minimum Principal Stress

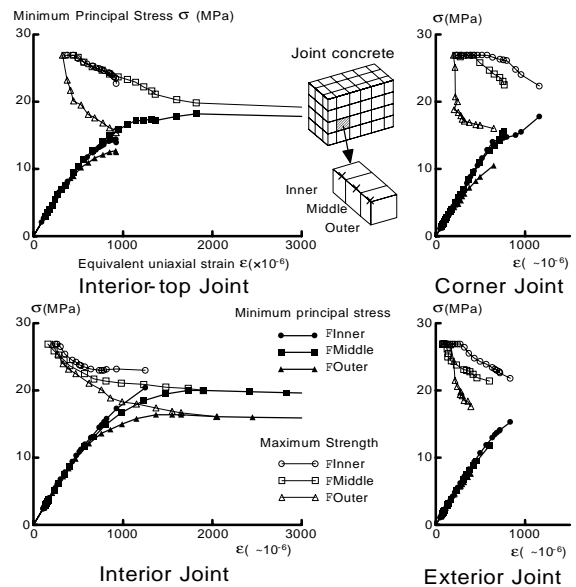


Figure 6: Minimum Principal Stress - Equivalent Uniaxial Strain Relationship

Deformation components

The deformation components were calculated from the analytical results using the estimation method proposed by Sakaguchi [Sakaguchi, 1991] as shown in Figure 7. The torsional deformation components (α and β) between the outer panel and the inner panel accounted for the greater part of the panel deformation of beam-column joints as shown in Figure 8.

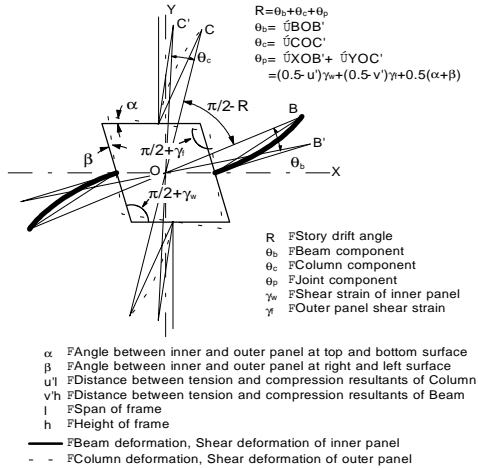


Figure 7: Deformation Components

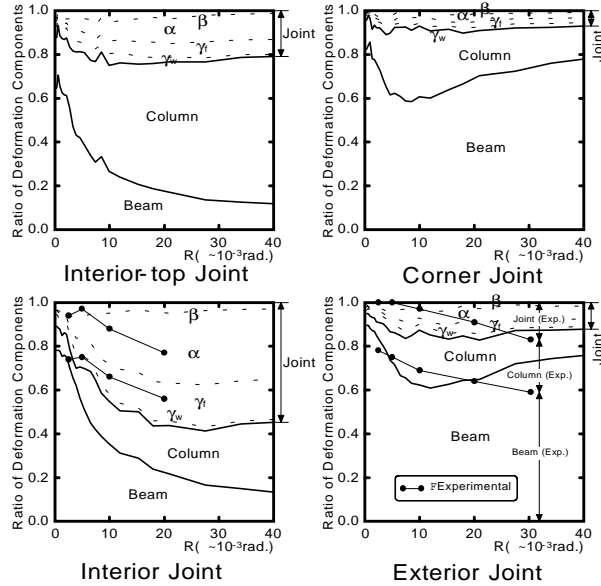


Figure 8: Ratios of Deformation Components

Joint shear force-shear strain relationship

Joint shear force that was difficult to estimate from experimental results was calculated from the analytical results directly. The total of the equivalent nodal forces which are transferred across the mid-plane of the beam-column joint in the X direction is defined as the joint shear forces shown in Figure 9. Joint shear force-shear strain relationships are shown in Figure 10. The shear strengths that are calculated by three equations that proposed by Kim-Noguchi [Kim, 1998], Sakaguchi [Sakaguchi, 1991] and JCI [Japan Concrete Institute, 1991] are indicated in Figure 10. The shear strength of the interior beam-column joint obtained by the FEM analysis agrees with three calculated shear strengths.

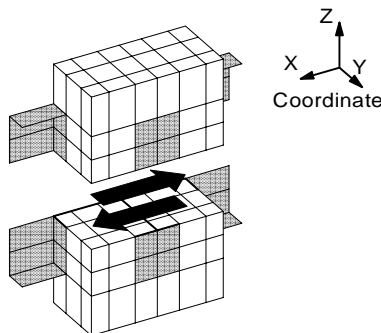


Figure 9: Joint Shear Force

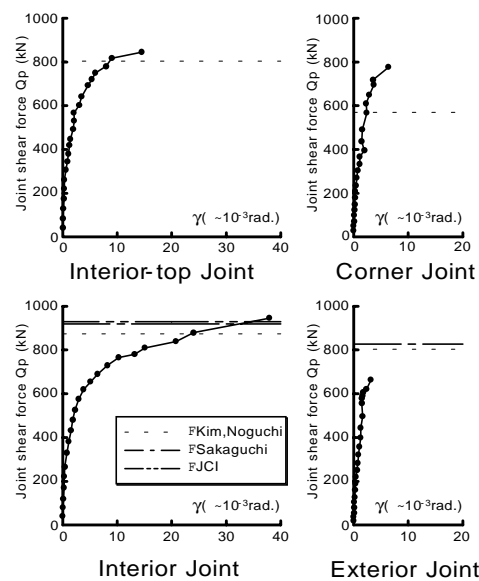


Figure 10: Joint Shear Force - Shear Strain Relationship

Contribution of shear resisting components

The beam-column joint is divided into five shear resisting components such as a steel web, inner concrete, middle concrete, outer concrete and an FBP as shown in Figure 11. The shear force of each component is calculated from each total equivalent nodal force. The ratios of shear resisting components are shown in Figure 12.

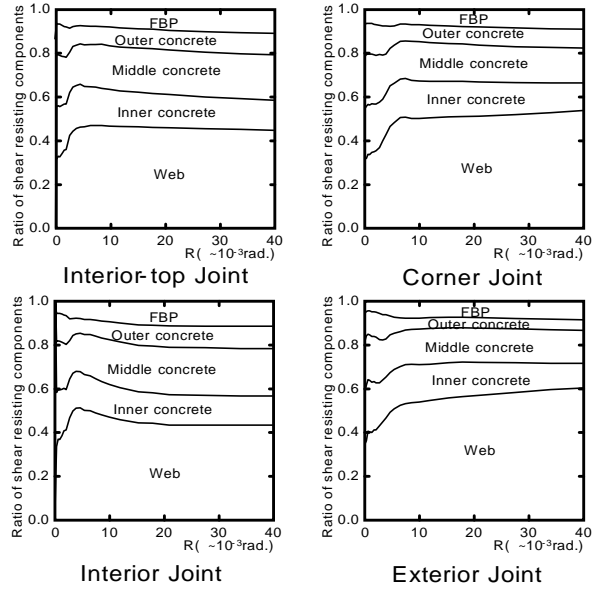
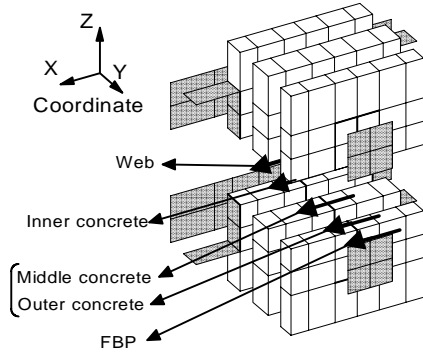


Figure 11: Shear Resisting Components

Figure 12: Ratios of Shear Resisting Components

The contributing shear force of the FBP accounts for about 10% of the total. The previous shear strength equations are based on the superposed shear strength of the steel web and the joint concrete. Each equation can be expressed as the following common expression in order to compare the components of three previous equations and those of FEM analytical results.

$$Q_p = k_w \frac{\sigma_{wy}}{\sqrt{3}} A_w + k_{c1} 0.3 \sigma_B A_{c1} + k_{c2} 0.3 \sigma_B A_{c2} + k_f \frac{\sigma_{fy}}{\sqrt{3}} A_f \quad (1)$$

Web *Inner Concrete* *Outer Concrete* *FBP*
 k_w, k_{c1}, k_{c2}, k_f : Effective coefficient A_w, A_{c1}, A_{c2}, A_f : Section Area
 σ_{wy}, σ_{fy} : Yield strength σ_B : Compressive strength

Comparison of the effective coefficients of the interior beam-column joint is shown in Table 1. The shear capacities of the three equations and the FEM results are similar, but the effective coefficients are different. The factor of FBP is not considered in any equations.

Table 1: Comparison of Effective Coefficients

	Effective coefficient				$\frac{Q_{FEM}}{Q_{CAL}}$
	Steel	Concrete		FBP	
		Inner	Outer		
FEM	0.63	0.54	0.61	0.20	
Kim, Noguchi	0.83	1.0	0.19		1.08
Sakaguchi	0.81	0.54	0.54		1.03
JCI	1.0	0.39	0.39		1.02

ANALYSIS OF FRAME SPECIMEN WITH COVER PLATES

Reference Specimen

Specimen OIT that had two stories and two spans was tested by Nishimura et al [Nishimura, 1998] in U.S. - Japan cooperative research program. The joint detail was a beam through type with cover plates and steel bands. The test specimen was designed to cause the beam yielding and the shear failure of beam-column joints at the same time. Axial loads were applied to the top of each column. Cyclic reversal lateral loads were applied to the beam end of the two stories. It was reported that concrete crush around the beam - column joints was observed remarkably. The shape of specimen is shown in Figure 13.

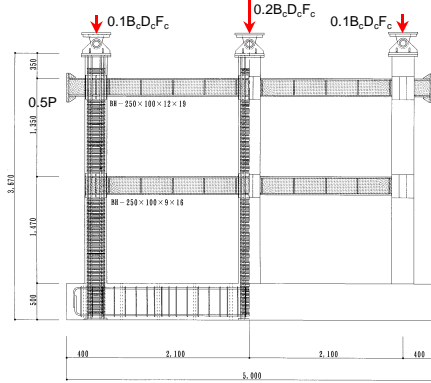


Figure 13: Shape of Specimen OIT

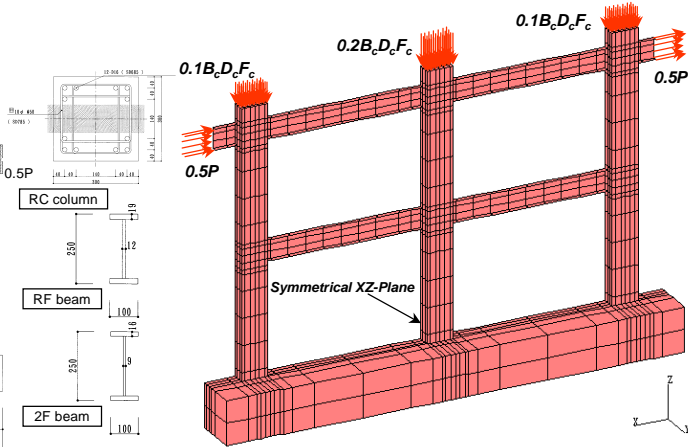


Figure 14: Finite Element Idealization

Modeling of Specimen

The finite element idealization of the specimen OIT is shown in Figure 14. Half part of the specimen including the stub was modeled by using the symmetrical condition at the center in the direction of width. The modeling of the beam-column joints is shown in Figure 15. The details of the beam-column joints are modeled approximately with actual ones. In the analysis, bond elements were used between elements of reinforcing bars and concrete elements, and interface elements were used between steel shell elements and concrete elements. Pulling out of column re-bars from the stub were considered by using bond link elements. Axial loads were applied to the top of the columns, and monotonic lateral loads were applied to the beams of the roof story in the analysis.

This was prediction analysis before the test. Because the actual material properties were not obtained at the analysis, the material properties listed in Table 2 were assumed. Table 2 shows the comparison of actual and assumed material properties. The measured compressive strength of the concrete and yield strength of the steel, which had a big influence on the behaviors of the test specimen, were close to the assumed values.

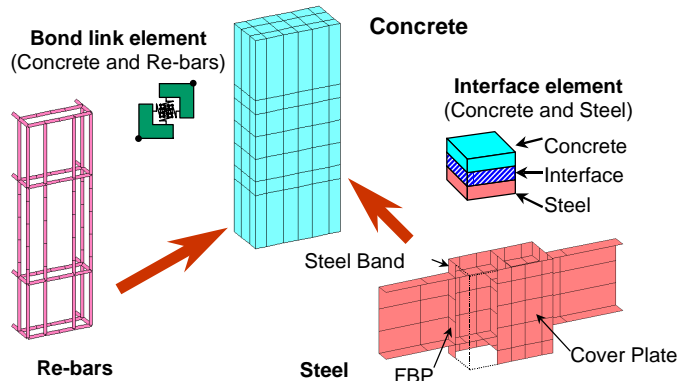


Figure 15: Modeling of Beam-Column Joint

Table 2: Comparison of Assumed and Measured Material Properties

	Test	FEM
Concrete		
Young's Modulus		2.17×10^4 (MPa)
Compressive Strength	27.1	26.5 (MPa)
Strain at Comp.Strength		2.06×10^{-3}
Tensile Strength	2.52	1.93 (MPa)
Steel		
Young's Modulus		2.06×10^5 (MPa)
Yield Strength		
PL2.3 (SS400)	351.8	258.9 (MPa)
PL3.2 (SS400)	347.7	258.9 (MPa)
PL 6 (SS400)	252.9	258.9 (MPa)
PL 9 (SM490)	377.9	356.0 (MPa)
PL12 (SM490)	399.9	356.0 (MPa)
PL16 (SM490)	387.4	356.0 (MPa)
PL19 (SM490)	357.1	356.0 (MPa)
Re-bar		
Young's Modulus		2.06×10^5 (MPa)
Yield Strength 10# (SD785)	884.1	785 (MPa)
D16 (SD685)	758.7	685 (MPa)

Analytical Results and Discussions
Load-Deflection Relationship

The relationships between load and deformation are shown in Figure 16. The load is the lateral load applied to the beams of the roof story. The deformation is the lateral deformation angle between the center in the beam-column joint of the roof story central column and the basement. From the comparison of experimental and analytical results, the analytical result was able to predict the load-deflection relationship and the maximum strength of the test specimen successfully. In the test results, the capacity was kept to the lateral deformation angle of $R=40/1000$ rad. After that the load decreased. In the analysis, the answer was not obtained after $R=30/1000$ rad. from no convergence during iteration process due to the load control.

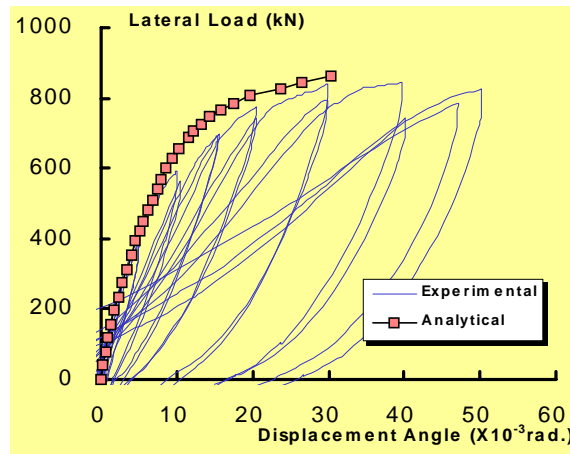


Figure 16: Load – Deflection Relationship

Failure characteristics

Figure 17 illustrates the deformation pattern and the process of yielding occurrence. It was found visually that the shear deformation of the beam-column joints was remarkable. The process of the failure in the analysis was the following order : (a) the web of beam-column joints of the roof story, (b) flexural yielding of the beam flanges of second story, (c) tensile and compressive yielding of the reinforcing bars of the bottom of the first floor column, (d) flexural yielding of the beam flanges of the roof story, (e) tensile yielding of the reinforcing bars of the top of the second floor central column.. This process will be compared with the experimental results. The last failure situation of the test results is shown in Figure 18. The locations of concrete crush of analytical results are shown in Figure 19. The symbol of ● in Figure 19 indicates that the minimum principal strain exceeds the maximum strain in the stress-strain relationship at the integral points of concrete elements. From the comparison of Figures 16 and 17, it is found that the failure zone of the test results corresponds to the concrete crush zone of the analytical results.

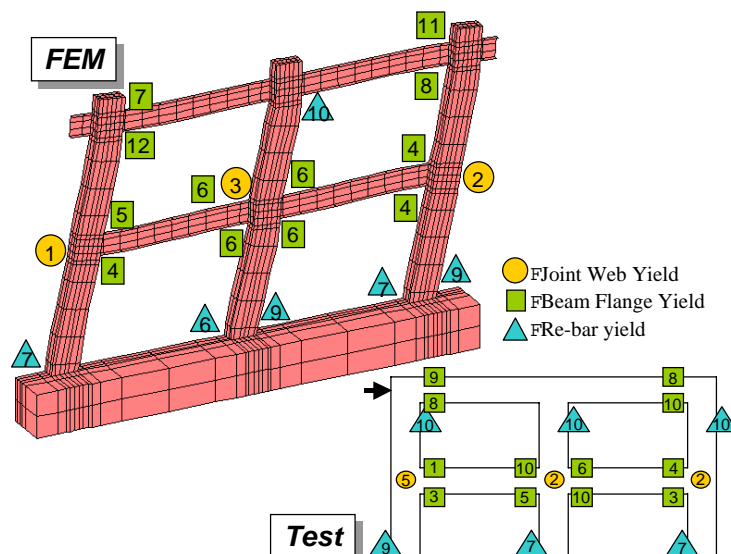


Figure 17: Deformation Pattern and Failure Process

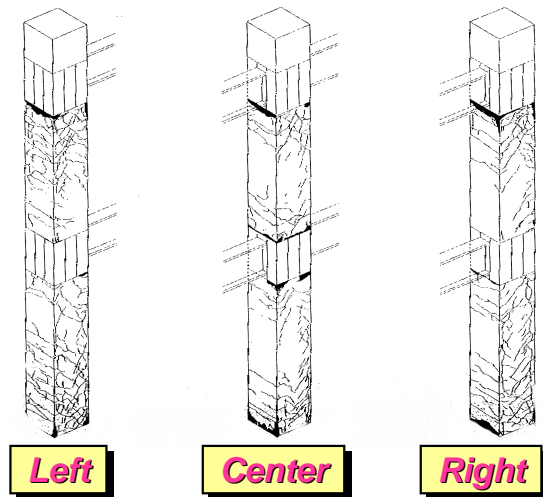


Figure 18: Last Failure Situation of Test

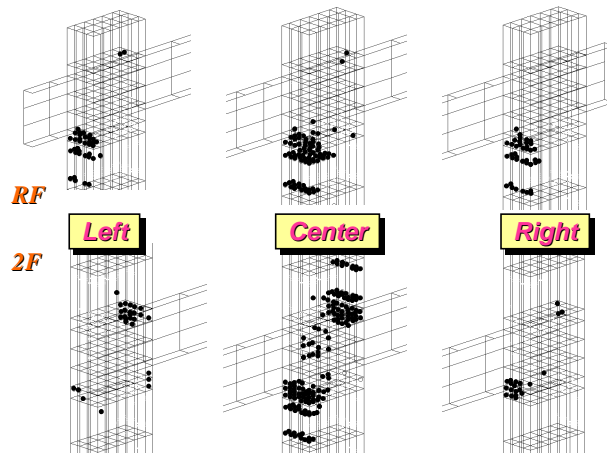


Figure 19: Locations of Concrete Crush of FEM

CONCLUSIONS

In this research, the nonlinear 3-D finite element analysis of a frame specimen with R/C columns and steel beams has been conducted. From the 3D-FEM analytical results, the following conclusions were obtained.

- (1) The 3D-FEM analysis considering the interaction between reinforcing bars and concrete and between steel and concrete simulated the behaviors of RCS frame specimens well.
- (2) A compressive strut was formed from outer concrete to inner concrete in the joint area divided by the transverse beams.
- (3) The torsional deformation component between an outer panel and an inner panel accounted for the greater part of the panel deformation of beam-column joints.
- (4) The ratios of the shear resisting components that were assumed in the proposed equations of the ultimate shear strength for interior beam-column joints were different from the ratios that were obtained from the FEM analytical results.
- (5) The failure characteristics obtained from the analysis corresponded to the observation in the test.

REFERENCES

- Iizuka, S., Kasamatsu, T. and Noguchi, H. (1997), "Study on The Aseismic Performance of Mixed Framed Structures", Journal of Structural and Construction Engineering, AIJ, No.497, 189-196 (in Japanese).
- Japan Concrete Institute (1991), "The Report of the Research Committee of Hybrid Structures", JCI (in Japanese).
- Kim, K. and Noguchi, H. (1998), "A Study on The Ultimate Shear Strength of Connections with RC Columns and Steel Beams", Journal of Structural and Construction Engineering, AIJ, No.507, 163-169 (in Japanese).
- Nishimura, Y., Kojima, T. and Baba, N. (1998), "U.S.-Japan Cooperative Research Project on Composite and Hybrid Structures (RCS-34 : Elastic-Plastic Behaviors RCS Composite Frame (Part 1)), Summaries of Technical Papers of Annual Meeting Architectural Institute of Japan, C-1, 1281-1282 (in Japanese).
- Sakaguchi, N. (1991), "Shear Force-Deformation Curves of Beam-Column Joint in Structural Frame Composed of Steel Beams and Reinforced Concrete Columns", Journal of Structural and Construction Engineering, AIJ, No.429, 55-64 (in Japanese).
- Uchida, K. , Mikame, A. and Noguchi, H. (1994), "Three-Dimensional Nonlinear Finite Element Analysis of Connections between Steel Beams and Reinforced Concrete Columns in Hybrid Structures", Computational Structural Engineering for Practice, Civil-Comp Press, 143-150.
- Uchida, K. and Noguchi, H. (1998), "Analysis of A Two Story, Two Bay Frame Consisting of Reinforced Concrete Columns and Steel Beams with Trough-Beam Type Beam-Column Joints", Journal of Structural and Construction Engineering, AIJ, No.514, 207-214 (in Japanese).